Received: 21 April 2020 | Revised: 14 August 2020 | Accepted: 20 August 2020

DOI: 10.1111/mec.15626

ORIGINAL ARTICLE

MOLECULAR ECOLOGY WILEY

Little genetic structure in a Bornean endemic small mammal across a steep ecological gradient

Lillian D. Parker[1,2] | Melissa T. R. Hawkins[1,3,4] | Miguel Camacho-Sanchez[5] | Michael G. Campana[1,2,4] | Jacob A. West-Roberts[1,6] | Tammy R. Wilbert[1] | Haw Chuan Lim[1,2] | Larry L. Rockwood[2] | Jennifer A. Leonard[5] | Jesús E. Maldonado[1,2,4]

[1]Center for Conservation Genomics, Smithsonian Conservation Biology Institute and National Zoological Park, Washington, DC, USA

[2]School of Systems Biology, George Mason University, Fairfax, VA, USA

[3]Division of Mammals, Department of Vertebrate Zoology, National Museum of Natural History, Smithsonian Institution, Washington, DC, USA

[4]Department of Environmental Science and Policy, George Mason University, Fairfax, VA, USA

[5]Conservation and Evolutionary Genetics Group, Estación Biológica de Doñana (EBD-CSIC), Seville, Spain

[6]Department of Computational Biology, Carnegie Mellon University, Pittsburgh, PA, USA

Correspondence
Lillian D. Parker, Center for Conservation Genomics, Smithsonian Conservation Biology Institute and National Zoological Park, Washington, DC, USA.
Email: parkerld@si.edu

Funding information
National Science Foundation, Grant/Award Number: 1547168 and 1717498; Ministerio de Economía y Competitividad, Grant/Award Number: CGL2010-21524 and CGL2017-86068-P; College of Science, George Mason University; Smithsonian Institution

Abstract

Janzen's influential "mountain passes are higher in the tropics" hypothesis predicts restricted gene flow and genetic isolation among populations spanning elevational gradients in the tropics. Few studies have tested this prediction, and studies that focus on population genetic structure in Southeast Asia are particularly underrepresented in the literature. Here, we test the hypothesis that mountain treeshrews (*Tupaia montana*) exhibit limited dispersal across their broad elevational range which spans ~2,300 m on two peaks in Kinabalu National Park (KNP) in Borneo: Mt Tambuyukon (MT) and Mt Kinabalu (MK). We sampled 83 individuals across elevations on both peaks and performed population genomics analyses on mitogenomes and single nucleotide polymorphisms from 4,106 ultraconserved element loci. We detected weak genetic structure and infer gene flow both across elevations and between peaks. We found higher genetic differentiation on MT than MK despite its lower elevation and associated environmental variation. This implies that, contrary to our hypothesis, genetic structure in this system is not primarily shaped by elevation. We propose that this pattern may instead be the result of historical processes and limited upslope gene flow on MT. Importantly, our results serve as a foundational estimate of genetic diversity and population structure from which to track potential future effects of climate change on mountain treeshrews in KNP, an important conservation stronghold for the mountain treeshrew and other montane species.

KEYWORDS

conservation genetics, elevational range, mitogenomes, mountain treeshrews, population genomics, ultraconserved elements

1 | INTRODUCTION

Tropical ecosystems are global hotspots of biodiversity and endemism. To explain the higher diversity in lower latitude regions, Janzen (1967) proposed that the greater temporal thermal stability and spatial environmental heterogeneity on tropical mountains should select for narrow thermal tolerances, which in turn reduce effective dispersal and increase population isolation across elevational gradients (Ghalambor et al., 2006; Gill et al., 2016). Numerous studies support the first prediction of the hypothesis that species in the

Parker and Hawkins are first authors.

tropics have narrower elevational ranges than those in the temperate zone (Ghalambor et al., 2006; McCain, 2009). Fewer studies have tested the second prediction that restricted gene flow among populations spanning elevational gradients results in genetic divergence (Ghalambor et al., 2006). Available data regarding this prediction are contradictory: some studies have found significant population genetic divergence across elevations, for example in insects (Gueuning et al., 2017; Polato et al., 2018) and in endotherms including birds (Bertrand et al., 2014; DuBay & Witt, 2014; Gadek et al., 2018; Linck et al., 2019) and mammals (Feijó et al., 2019). Others have detected high rates of gene flow alongside adaptive phenotypic divergence (Branch et al., 2017; Cheviron & Brumfield, 2009).

Few studies have investigated the spatial population genetic structure of small mammals across elevational gradients in tropical montane ecosystems (Muenchow et al., 2018). Thus, the influence of elevational gradients on gene flow in terrestrial endotherms at small spatial scales is not well understood. Studying spatial population genetic structure in the montane tropics is important not only because it allows for hypothesis testing regarding the effects of elevational gradients on genetic structure, but also because it enables researchers to identify distinct evolutionary units warranting protection and to establish benchmarks from which to monitor responses to changing global environmental conditions (Camacho-Sanchez et al., 2018; Castillo Vardaro et al., 2018; Moritz, 1994). This is critical given the vulnerability of tropical montane ecosystems to the impacts of global climate change (GCC) (Feeley et al., 2017; Lenoir & Svenning, 2015).

Here, we investigate the genetic structure of the mountain treeshrew, *Tupaia montana*, across its full elevational range on two mountains in Kinabalu National Park (KNP), Sabah, Borneo: Mt Kinabalu (MK) and Mt Tambuyukon (MT; Figure 1). The mountain treeshrew provides an interesting system in which to study the effect of environmental gradients on population structure because it has a broad elevational distribution compared to other small mammals in KNP (Camacho-Sanchez et al., 2019; Nor, 2001). On MK, the species occurs from ~900 m above sea level (masl) to at least 3,200 masl, encompassing four vegetation zones; on MT it ranges from ~900 m to the summit at 2,579 masl, including three vegetation zones (Kitayama, 1992). Given the temperature lapse rate in KNP at −0.55°C per 100 m of elevation gain (Kitayama, 1992),

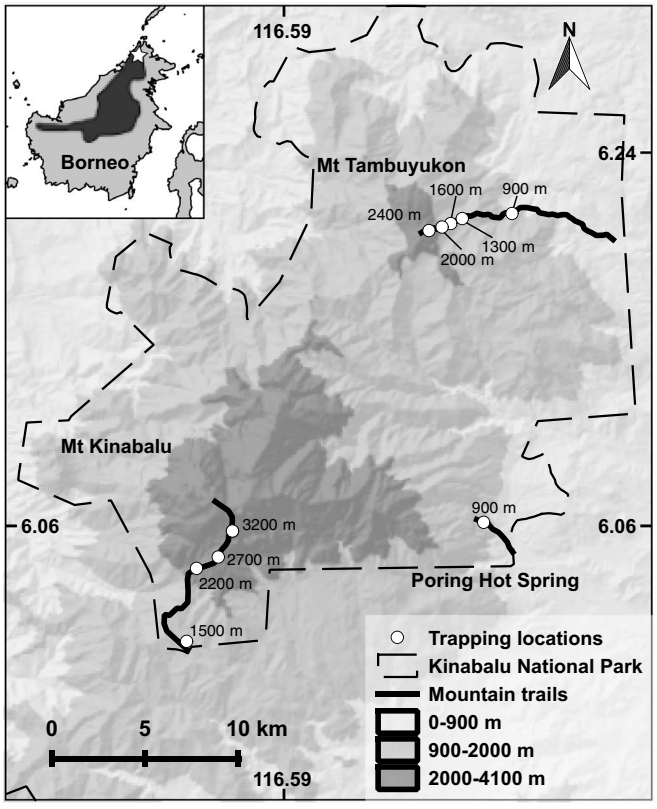

FIGURE 1 (a, left) Map of mountain treeshrew distribution (inset modified from IUCN 2019, with a white star indicating the location of Kinabalu National Park, KNP), and a map of sampling locations within KNP, Sabah, Borneo. Park boundaries are demarcated by dashed lines, transects by black lines and sampling locations by white circles, with elevations at each site labelled. Shading indicates the lower and upper portions of mountain treeshrew habitat, with 900–2,000 masl shown in medium grey and >2,000 masl in dark grey. The total number of mountain treeshrews collected and the number of unrelated individuals included in our analyses at each trapping site are as follows (unrelated/total): MK 900, 6/6; 1,600 5/6; 2,200 5/5; 2,700 4/4; 3,200 5/5; MT 900 4/4; 1,300 4/6; 1,600 4/4; 2,000 14/22; 2,400 7/14. (b, right) Image of a mountain treeshrew and a pitcher plant (*Nepenthes lowii*), KNP (Photo credit: Chien C. Lee). The two species exhibit a mutualistic relationship in which mountain treeshrews feed on the sugary secretions provided by the plant and in turn provide the plant with phosphorous and nitrogen through faeces (Chin et al., 2010)

mountain treeshrews experience a 12.65°C average range in temperature on MK, which is higher than the thermal neutral zone for most small mammals (Khaliq et al., 2014). On MT, mountain treeshrews experience an 8.8°C temperature range (Camacho-Sanchez et al., 2018).

Mountain treeshrews exhibit facultative mutualism with pitcher plants in the genus *Nepenthes*—treeshrews consume the plants' carbohydrate-rich secretions and defecate into the pitchers, providing the plants with supplementary nitrogen and phosphorous (Chin et al., 2010; Clarke et al., 2009). Although mountain treeshrews provide critical nutrients to the plant, the importance of the plant to treeshrews is unknown. The range of mountain treeshrews exceeds that of the plants—none of the plants are distributed below 1,200 masl or above 2,650 masl. As such, treeshrews are not reliant on them for nutrients even in high-elevation areas without fruiting trees.

We test the hypothesis that, consistent with Janzen's (1967) hypothesis, restricted gene flow across the steep ecological gradient that mountain treeshrews inhabit has resulted in significant genetic differentiation. Although the ecology of mountain treeshrews is poorly understood, our hypothesis is informed by observations of small home ranges (Emmons, 2000; Payne et al., 2016) and phenotypic changes associated with elevational changes (Hinckley et al., in review). We predict that mountain treeshrews will exhibit significant differentiation in neutral genetic markers (i) between mountains, due to limited dispersal across the lowland habitat that connects them, and (ii) across elevations—with greater differentiation on MK due to its higher elevation and associated environmental variability.

To test our predictions, we analyse both mitochondrial genomes (mitogenomes) and nuclear ultraconserved element (UCE)-associated single nucleotide polymorphism (SNP) markers from mountain treeshrews collected across their full elevational range in KNP in a population genetics framework. Previous studies have shown that UCEs are sufficiently variable to resolve shallow phylogenies on a phylogeographical scale (Faircloth et al., 2012; Harvey et al., 2016; Mason et al., 2018; Smith et al., 2014) including intraspecific phylogenies (Giarla et al., 2018), and to answer questions regarding recently diverged species (Oswald et al., 2016; Winker et al., 2018). However, ours is one of the first studies to describe the intraspecific variability of SNPs derived from UCE loci at a fine spatial scale.

2 | MATERIALS AND METHODS

2.1 | Sample collection

We trapped small mammals on both MK and MT within KNP (6°09′N, 116°39′E) during two field seasons in 2012 and 2013. At 4,095 masl, MK is the tallest mountain in the Sundaland biogeographical region. It is relatively young, having reached its present height ~1 million years ago (Ma) (Hall et al., 2009). Eighteen kilometres to the north of MK, the less-studied MT stands at 2,579 masl (Figure 1a). MT is older—its major uplift occurred as part of a different geological process, as part of the Crocker Range, 7–11 Ma (Hall et al., 2009).

Our trapping methodology and permitting information is described in Camacho-Sanchez et al. (2019). Briefly, we set traps from ~503 to 3,466 masl on MK and from ~331 to 2,509 masl on MT (Figure 1a). The mountain treeshrew was the most frequently caught species, representing 37.5% of all catches. For this study, we included 92 *Tupaia* individuals: 84 mountain treeshrews and eight outgroup individuals from three congeners, the pygmy treeshrew (*T. minor*, $n = 2$), the large treeshrew (*T. tana*, $n = 5$) and the ruddy treeshrew (*T. splendidula*, $n = 1$), the sister species of the mountain treeshrew (Roberts et al., 2011; Table S1).

2.2 | Laboratory methods

Laboratory work was performed at the Center for Conservation Genomics (CCG), Smithsonian Conservation Biology Institute, Washington, DC. We extracted DNA from liver and ear punch samples using a DNeasy Blood and Tissue Kit (Qiagen) following the manufacturer's protocol. We amplified whole mitogenomes in two fragments using long-range PCR (polymerase chain recation), fragmented the PCR products to an average length of 500 bp using a Qsonica Q800R sonicator (QSonica), and prepared single-indexed DNA libraries for sequencing using a Kapa LTP Library Preparation kit (Kapa Biosystems) following Hawkins et al. (2016). We pooled libraries equimolarly and sequenced on an Illumina MiSeq with 2 × 100-bp reads (Illumina).

We used in-solution DNA hybridization to enrich genomic DNA for UCEs following Hawkins et al. (2016). We sheared DNA extracts and constructed indexed libraries as above. We quantified libraries using a Qubit fluorometer (Life Technologies) with a 1× double-stranded DNA HS assay kit and multiplexed four to eight samples equimolarly prior to enrichment. We used a NimbleGen SeqCap EZ kit (Roche) containing 54,689 unique 60-bp DNA probes representing 5,561 vertebrate UCE loci with an average of 4× tiling per base per locus to enrich multiplexed libraries following the manufacturer's protocol. Post-enrichment libraries were amplified with 12–14 cycles of PCR using Kapa HiFi HotStart DNA polymerase (Kapa Biosystems) following the manufacturer's protocol.

Following visualization on a Bioanalyzer 2100 (Agilent Technologies) with High Sensitivity DNA kits, enriched libraries were quantified via quantitative PCR (qPCR) using the Kapa Biosystems Illumina Library Quantification Kit (Kapa Biosystems). Samples were pooled equimolarly and sequenced with 2 × 150-bp reads on Illumina HiSeq2000 (Semel Institute of Neurosciences, UCLA, and University of Copenhagen, Denmark) and MiSeq (CCG) platforms.

2.3 | Mitogenome assembly and alignment

We analysed mitogenomes to investigate the population structure and genetic diversity of mountain treeshrews. Because mitogenomes are inherited matrilineally and are not subject to recombination, they are frequently used to investigate population structure, colonization history and species' demographic histories (Harrison, 1989).

Mitogenome amplicon reads were quality filtered with TRIMMOMATIC version 0.33 (Bolger et al., 2014) with parameters SLIDINGWINDOW: 4:15 and MINLEN: 36. Because the only publicly available mitogenome representing any *Tupaia* species (the northern treeshrew, *T. belangeri* NC_002521; Schmitz et al., 2000) is highly divergent from our study species (Roberts et al., 2011), we first generated reference mitogenomes for the mountain treeshrew and three closely related outgroup species: the pygmy treeshrew, large treeshrew and ruddy treeshrew. For each species, we selected one individual with the highest number of sequencing reads (pygmy treeshrew, BOR 443; large treeeshrew, BOR 010; ruddy treeshrew, UMMZ174429) and assembled sequences de novo with the MIRA version 1.0.1 plugin in GENEIOUS version 9.1.2 (Biomatters), using "Quality Level Accurate" and default settings. Quality filtered sequence reads were mapped to the appropriate reference using BWA-MEM version 0.7.10 (Li, 2013) with default parameters. We also assembled mitogenomes from UCE-enriched library sequences (Supporting Information). Consensus sequences were generated with GENEIOUS (lowest coverage to call a base 5× and Highest Total Quality parameters) and aligned with the MAFFT version 7.450 plugin (Katoh et al., 2002). We transferred annotations from the northern treeshrew reference to the consensus sequences. To rule out the presence of nuclear copies of mitochondrial genes (NUMTs), we translated all protein-coding genes to check for frame shifts or stop codons.

2.4 | Genetic diversity and population structure

Because the inclusion of close relatives can bias estimates of genetic diversity and structure (Goldberg & Waits, 2010), we removed first-order relatives identified by our SNP data set and performed all subsequent mitogenome analyses with the reduced data (hereafter "unrelated data set"). We defined haplotypes and calculated haplotype diversity (H_d), nucleotide diversity (π) and Tajima's *D* using DNASP version 6.12.03 (Librado & Rozas, 2009). We estimated the differentiation between MK and MT and between high and low elevations within each peak through analysis of molecular variance (AMOVA) in ARLEQUIN version 3.5 (Excoffier & Lischer, 2010) with a permutation test of 10,000 replicates to assess statistical significance. We visualized relationships among haplotypes by generating a median-joining network with POPART version 1.7 (Leigh & Bryant, 2015).

2.5 | Phylogenetic analysis and modelling demographic history

We performed phylogenetic analyses to place the mitochondrial lineages detected in our mountain treeshrew samples within an evolutionary framework with respect to other Bornean treeshrew species in the *Tupaia* clade (i.e., the large treeshrew, pygmy treeshrew and ruddy treeshrew), and to confirm the monophyly of the mountain treeshrew within the group. We used PARTITIONFINDER version 2.0 (Lanfear et al., 2012) to select partitions and substitution models and estimated a phylogeny using MRBAYES version 3.2.6 (Ronquist & Huelsenbeck, 2003). We then used BEAST version 1.8.4 (Drummond & Rambaut, 2007) to estimate the timing of divergence between the mountain treeshrew mitochondrial lineages we identified.

To infer demographic history, we performed a Bayesian coalescent skyline plot analysis using BEAST version 2.0 (Bouckaert et al., 2014). We used a time to most recent common ancestor (TMRCA) prior of 450,000 years before present (lognormal distribution, $\mu = 0.45$, $\sigma = 0.2$), the estimated date of divergence between the two mitochondrial lineages as determined by the dating analysis performed in BEAST (Supporting Information).

2.6 | Genotyping UCE-associated SNPs

To generate the SNP data set, we followed the PHYLUCE version 1.5.0 pipeline with default parameters (Faircloth, 2016) for sequence trimming, de novo assembly of contigs, identification of UCE loci, and sequence alignment. We generated a pseudogenomic reference by aligning each locus with MAFFT version 7.407 and trimming using GBLOCKS version 0.91b with default parameters (Castresana, 2000). We then used GENEIOUS to generate a consensus sequence for each locus, replacing ambiguity codes with an appropriate nucleotide at random. We used PICARD version 1.106 (http://broadinstitute.github.io/picard/), and SAMTOOLS version 1.9 (Li et al., 2009) to create sequence dictionaries and reference indices from the reference. We used the PHYLUCE script *snps.py* to automate alignment of trimmed reads from each sample to the reference with BWA-MEM version 0.7.17, and then called SNPs with the HaplotypeCaller tool of the Genome Analysis Toolkit version 3.7 (GATK; McKenna et al., 2010) following Giarla and Esselstyn (2015). Using VCFTOOLS version 0.1.16 (Danecek et al., 2011), we removed SNPs that failed to pass GATK quality filters (QD < 2.0 || FS > 60.0 || MQ < 40.0 || HaplotypeScore > 13.0 || MappingQualityRankSum < −12.5 || ReadPosRankSum < −8.0), and selected SNPs with a minimum depth of coverage of 8 per individual and a minor allele frequency ≥ 5%. We used *HD_plot.py* (McKinney et al., 2017) to filter SNPs resulting from putative paralogues or incorrectly assembled contigs from the data set by removing SNPs with heterozygosity >0.75 and a read-ratio deviation score D >10. The D statistic is a measure of deviation from the expected allelic read ratio of 1:1 when reads are summed over all heterozygous individuals. This method more accurately identifies true

SNP loci than methods relying on read depth or heterozygote excess alone (McKinney et al., 2017). After filtering with *HD_plot.py*, we further filtered SNPs that that were out of Hardy–Weinberg equilibrium (HWE) after Bonferroni correction for multiple comparisons ($p < 10^{-5}$) using VCFTOOLS version 0.1.16 because strong deviations from HWE are usually indicative of genotyping error (Chen et al., 2017). To generate a set of unlinked SNPs, we selected one SNP per UCE using VCFTOOLS version 0.1.16 "-thin 2000." We used the unlinked SNP data set with 10% missing data for all SNP-based analyses except calculation of genetic diversity and effective population size, principal components analysis (PCA), discriminant analysis of principal components (DAPC) and Bayesian cluster analysis with STRUCTURE version 2.3.4 (Pritchard et al., 2000), for which we used a data set with no missing data.

2.7 | Generating phased pseudo-haplotype sequences

To include multiple SNPs per UCE locus as well as invariant sites for the MIGRATE-N analysis, we generated multiple sequence alignments of pseudohaplotypes. We did this by using the EMIT_ALL_SITES output mode of the GATK HaplotypeCaller tool. We filtered the resulting VCF file to include only UCE loci with at least one SNP with no more than 10% missing data. We then generated alignments from the VCF file with a custom RUBY script, *vcf2aln* version 0.4.2 (https://github.com/campanam/vcf2aln, Supporting Information). This script utilizes phasing information where present and randomly selects an allele where phase is unresolved.

We trimmed the phased UCE sequence alignments with GBLOCKS version 0.91b (Castresana, 2000) using default parameters and quantified informative sites with the *phyluce_align_get_informative_sites.py* PHYLUCE script. For the final data set used in the MIGRATE-N analysis, we retained only loci with at least one and fewer than 10 parsimony-informative sites (PIS) to increase the signal-to-noise ratio of our data set. MIGRATE-N calculates model and parameter likelihoods for each locus independently and averages results across loci taking into account the posterior distributions of each (Beerli & Palczewski, 2010). Uninformative loci with flat posterior distributions contribute less to the final average; therefore, removing invariant loci should not bias our results, while including them increases computation time. We removed loci with more than 10 PIS (i.e., more than ~2*SD* above the mean [$\bar{x} = 3.6$, $SD = 4$]) because their diversity is probably artificially high due to errors introduced during de novo assembly or sequence alignment (Gilbert et al., 2018). Gilbert et al. (2018) showed that filtering sites on the basis of signal-to-noise in a concatenated UCE alignment improved the resolution of hard-to-resolve nodes in the Neoaves phylogeny, and that after filtration, the topology converged on that derived from a much larger data set.

2.8 | Genetic diversity and effective population size

We removed individuals that were identified as first-degree relatives (parent–offspring or full siblings) according to the KING version 2.1.4 software (Manichaikul et al., 2010; i.e., those with kinship coefficients ≥0.18). Using the unlinked SNPs with 10% missing data, we first calculated pairwise kinship values and identified putative family groups with the KING software and then ran a PC-AiR analysis with GENESIS version 2.2.2 (Conomos et al., 2016) in R version 3.6.3 (R Core Team 2019, applies to all subsequent use of R) to identify an "unrelated" subset of individuals. We used GENALEX version 6.503 to estimate the statistical power of the SNP data set to differentiate individuals by calculating p_{IDsib}, the probability of two individuals having identical genotypes assuming siblings are present in the data (Waits et al., 2001).

We calculated average expected and observed heterozygosity (H_E and H_O) and the inbreeding coefficient (F_{IS}) with VCFTOOLS version 0.1.16 using our SNPs with no missing data. We also concatenated FASTA alignments of UCE sequence pseudohaplotypes for all individuals in the unrelated data set and used the maximum composite likelihood method to calculate nucleotide diversity (π) in MEGA version 7.0.26 (Kumar et al., 2016).

We estimated effective population sizes (N_e) using the linkage disequilibrium model with random mating (Waples & Do, 2008) implemented in NEESTIMATOR version 2.1 (Do et al., 2014). We report estimated N_e values using "Lowest Allele Frequency Used" 5% and 95% confidence intervals generated by the "Parametric method" for unrelated individuals for each population cluster identified by STRUCTURE separately.

2.9 | Population structure

We characterized population genetic structure using the SNP data set with no missing data. We performed PCA and DAPC with the ADEGENET version 2.1.1 package (Jombart, 2008) in R. For the DAPC analysis, we first conducted *K*-means clustering and selected the number of clusters based on the lowest Bayesian information criterion (BIC) value. We performed cross-validation to determine the number of PCs to retain by calculating the lowest root mean squared error. We then ran DAPC, retaining 20 PCs and two discriminant functions.

We used STRUCTURE version 2.3.4 to infer the number of population clusters (K) and the proportion of individual membership assigned to each cluster (q_k). We used a burn-in of 500,000 steps followed by 1,000,000 recorded steps, tracking the probability of the data given K ($\ln P(D)$) to ensure that we ran the program long enough for the values to stabilize. We used the admixture model, no location priors and assumed correlated allele frequencies (Falush et al., 2003). We performed a simulation with K from 1 to 7 with 10 replicates each and identified meaningful K values using the ΔK method (Evanno et al., 2005) implemented in STRUCTURE HARVESTER version 0.6.94 (Earl & vonHoldt, 2012). We combined replicate runs using CLUMPP version 1.1.2 (Jakobsson & Rosenberg, 2007).

To quantify the levels of differentiation between population clusters identified by STRUCTURE, we performed an AMOVA and calculated pairwise F_{ST} values using the SNP data set with 10% missing

data in GENALEX version 6.5 (Peakall & Smouse, 2012), with 10,000 permutations to generate the null distribution. To investigate local spatial genetic structure, we performed a Mantel test using ADE4 version 1.7 (Dray & Dufour, 2007) in R on both the full and the unrelated data set. We tested for a correlation between pairwise genotypic distance and Euclidean geographical distance with 9,999 permutations to generate the null distribution. We also generated a Mantel correlogram to test for spatial autocorrelation between pairs of treeshrews at different distance classes using GENALEX. We first calculated pairwise linear geographical and genotypic distances, and then used the "Spatial" option with 9,999 permutations. We defined seven distance classes (0.2, 1.0, 2.0, 5.0, 10.0, 15.0 and 18.0 km) based on Sturges's Rule (Sturges, 1926), chosen to ensure sufficient comparisons within each class. Finally, we calculated the average, median and maximum geographical distances between pairs of individuals in each kinship class corresponding to first-, second-, third-order and distant relatives (Table 1) as an additional way to quantify the decay of genetic relatedness with distance. To test for significant differences between the means in each kinship class, we performed a one-way ANOVA in R with a Tukey Honest Significant Differences test and a Bonferroni correction for multiple comparisons (Combs et al., 2017).

2.10 | Migration and population models

We used the program MIGRATE-N version 3.6 with its Bayesian implementation (Beerli, 2005) to compare support for six different models of population structure and migration (diagrams of hypotheses in Figure 2). We used the phased pseudohaplotype sequence data set for this analysis to take advantage of the higher information content in DNA sequences relative to SNPs. Although our workflow may generate chimeric sequences in instances where phase is unresolved, we do not expect that this would affect model selection (Andermann et al., 2018; P. Beerli, pers. comm.). However, to ensure that phase did not affect model inference, we ran the MIGRATE-N analysis twice with different configurations of variants within haplotypes while maintaining all other settings.

We compared models to test our a priori hypotheses of significant genetic structure and limited gene flow between MK and MT and between high and low elevations. We also included models of population structure based on the STRUCTURE results in order to compare migration rates and directionality between population clusters. The models included the following: (i) panmixia, (ii) four populations (high-elevation MK, low-elevation MK, low-elevation MT and high-elevation MT) with bidirectional migration between adjacent pairs, (iii) three populations (high-elevation MT, low-elevation MT and all of MK) with bidirectional migration between adjacent pairs, (iv) three populations with migration between all pairs, (v) two populations (high-elevation MT separate from all others) with bidirectional migration, and (vi) two populations with unidirectional migration from high-elevation MT (Figure 2).

For model 2, we assigned individuals to populations based on their sampling location: low-elevation individuals <2,000 masl, and high elevation individuals ≥2,000 masl. For models 3, 4, 5 and 6, we assigned individuals based on STRUCTURE output for $K = 3$ and $K = 2$, respectively. We randomly selected five individuals from each population cluster ($n = 10$ haplotypes). We did not include all individuals because for coalescent processes, increasing the sample size above this does not necessarily improve accuracy, but substantially increases computation time (Felsenstein, 2005). For each model, we ran two long chains of 20,000,000 steps, sampled every 100 steps with 50,000 steps per chain discarded as burn-in, and with four heated chains. To ensure comparability across models, we ran the most complex model first and used the same prior distributions and ran parameters for all subsequent models. We assessed chain mixing through acceptance ratios and estimated sample size (ESS) of parameters and genealogies (ESS ≥ 40 million). We calculated log Bayes factors (LBFs) and model probability using the Bezier approximation of the marginal model likelihood and the formula described by Beerli and Palczewski (2010).

3 | RESULTS

3.1 | DNA sequencing

We obtained mitochondrial genome sequences from 83 mountain treeshrew individuals (MT423905–MT423940) and eight sequences from three congeners (MT442045–MT442052): the large treeshrew

TABLE 1 Geographical distances between pairs of individuals with different levels of estimated relatedness based on analysis with the KING software

Kinship	Relatedness	*n*	Average distance (m)	Median distance (m)	Maximum distance (m)
>0.18	First order (parent–offspring, siblings)	42	162.5	100.8	570.1
0.177–0.0884	Second order (e.g., half-siblings)	56	1,247	322.8	25,850
0.0883–0.0442	Third order (e.g., cousins)	112	4,819	793.0	26,490
<0.044	Distant or unrelated	2,932	12,310	15,960	29,430

Note: ANOVA and Tukey's Honest Significant Differences test showed significant differences in distances between all pairs except first- and second-order relatives and second- and third-order relatives ($p < .05$).

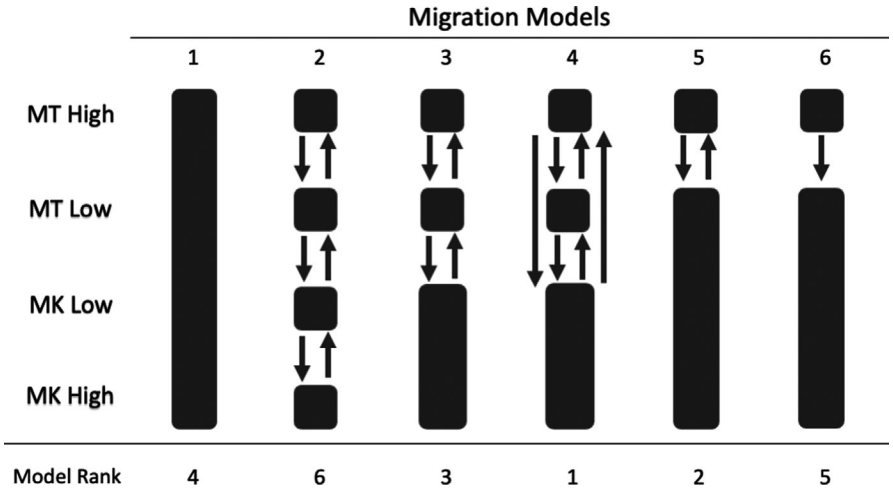

FIGURE 2 Population structure and migration models evaluated using MIGRATE-N, with model rank shown below each numbered model. The best model according to Bayes factors is model 4, followed by model 5. Log marginal likelihood values are listed in Table S5. MT, Mt Tambuyukon; MK, Mt Kinabalu; High, ≥2,000 masl; Low, <2,000 masl

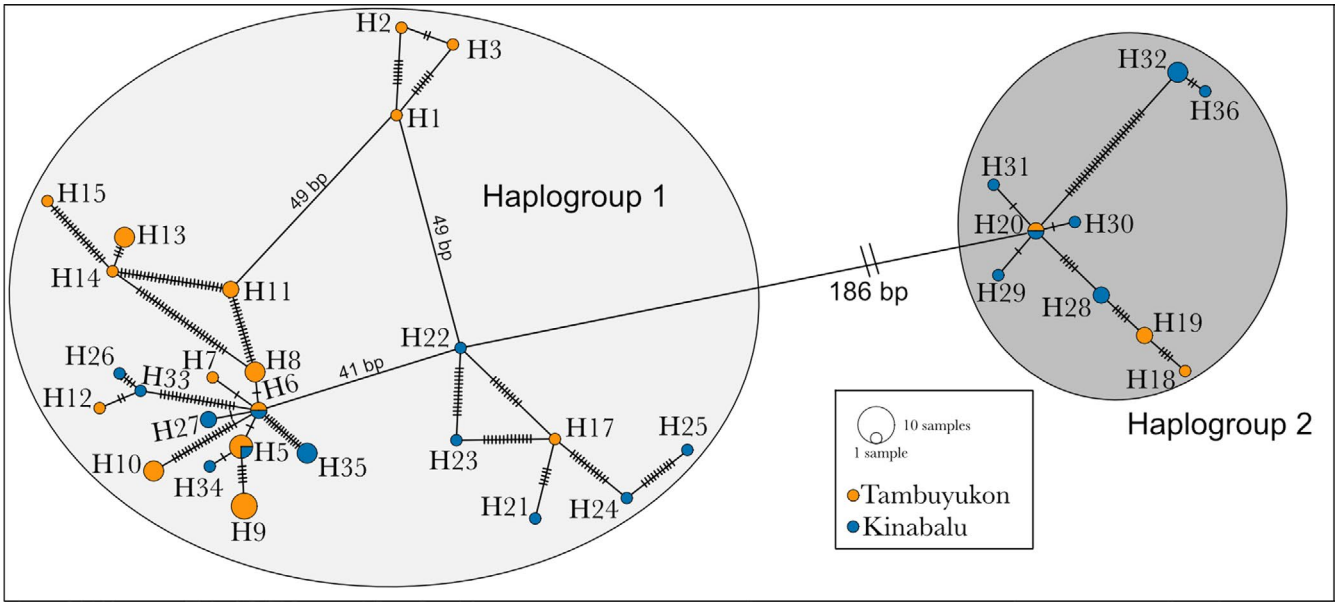

FIGURE 3 Median joining network of 34 mitogenome sequences in the "unrelated" data set. Haplotypes are numbered H1–H36; H4 and H16 are not included because they were removed when close relatives were trimmed from the data set. Dashed lines represent the number of base pair differences between haplotypes except in cases where the number of differences exceeds 40. Colours correspond to the two mountains (MT, orange; MK, blue). The two haplogroups are not shown to scale and are separated by 186-bp substitutions. Circle area is proportional to the number of individuals with each haplotype; the legend shows the size for one and 10 samples, respectively

(n = 5), the small treeshrew (n = 2) and the ruddy treeshrew (n = 1). Mitogenomes were sequenced to an average depth of 50×.

We sequenced UCEs from 80 mountain treeshrews (SRA accession PRJNA629376). Each UCE-enriched library was sequenced with a mean of 2.3 million reads (914,104–7,011,836), yielding a mean of 3,344 UCE loci (2,137–3,489) per sample. The total number of UCE alignments that we used to generate the pseudoreference was 4,106, and the mean length was 495 bp (149–2,167 bp). After aligning reads to the pseudoreference and quality filtering, there were 7,861 SNPs including multiple SNPs per locus. After removing loci with more than 10% missing data across individuals, 3,168 SNPs remained. The unlinked SNP data set included 1,794 independent SNPs. Removing loci with missing data left 684 unlinked loci. In the phased pseudohaplotype sequence alignment data set used for the MIGRATE-N analysis, 1,664 UCE alignments remained after removing loci with fewer than one (114 loci) and more than 10 PIS (16 loci; Figure S1).

3.2 | Mitogenomes: Genetic diversity, population structure and demographic inference

There were 36 unique mitochondrial haplotypes in the data set that included close relatives (n = 83), and 34 among the 58 unrelated individuals. All subsequent analyses were performed with the unrelated data set. H_d was high, at 0.977 (*SD* 0.008), and π was 0.00583 (*SD* 0.0006). Phylogenetic analyses show that mountain treeshrews are a monophyletic group with two deeply divergent lineages, each

present on both mountains (Figure S2, partitions and substitution models in Table S2). Outgroup relationships were consistent with the phylogenetic hypothesis presented by Roberts et al. (2011). The average number of nucleotide substitutions per site between the two lineages was 0.013. The BEAST dating analysis suggests that the two mitochondrial lineages diverged ~450,000 years ago (95% highest posterior density [HPD] 346,000–631,900 years ago, Figure S3).

The median joining haplotype network (Figure 3) shows that the two mountain treeshrew haplogroups are present on both MT and MK. Three haplotypes are found on both mountains (Table S3). Including related individuals, haplogroups 1 and 2 are found in near equal proportion on MK and MT (16 and 14 individuals, respectively), while haplogroup 1 is more frequent on MT (46 out of 53 individuals; Figure 4). The AMOVA on the unrelated data set showed significant differentiation between the two mountains ($F_{ST} = 0.133$, $p = .00812$), with 13.3% of the variance accounted for by differences between mountains and 86.7% within mountains. To test our prediction of significant differentiation across elevations, we then divided the population into high- (≥2,000 masl) and low- (<2,000 masl) elevation groups on each peak. The results showed that 90.42% of the total variance is accounted for by within-group variation, and 9.58% among-group variation ($F_{ST} = 0.096$, $p = .027$). Pairwise comparisons showed significant differences between high-elevation MK and low-elevation MT ($F_{ST} = 0.15$, $p = .023$) and high-elevation MK and high-elevation MT ($F_{ST} = 0.18$, $p = .013$); all other comparisons were not significant.

We performed Tajima's *D* test on an alignment including all unrelated individuals ($n = 57$) and separately on alignments with individuals from each haplogroup (haplogroup 1, $n = 43$; haplogroup 2, $n = 14$) and each mountain (MK, $n = 25$; MT, $n = 32$) because unaccounted for population structure can bias results even with high rates of migration among locations (Städler et al., 2009). In all cases the test was not significant, indicating a lack of evidence for recent population contraction, expansion, or selection. Similarly, in the Bayesian skyline plot analysis, the 95% HPD of the population change parameter included zero; therefore, we cannot reject the hypothesis of zero demographic changes in the last 60,000 years.

3.3 | UCE loci: Genetic diversity

Pairwise kinship calculations revealed several groups of putatively related individuals. After removing first-order relatives ($n = 22$ with kinship ≥0.18) from the data set, 58 individuals remained, including 33 from MT and 25 from MK. The nucleotide diversity of the filtered UCE pseudohaplotype alignment used in the MIGRATE-N analysis (1,664 concatenated UCE alignments) for all 58 unrelated mountain treeshrews was 0.0017 (*SE* 0.000022). The nucleotide diversity of the unfiltered alignment, including invariant loci and those with >10 PIS (3,935 UCE alignments) was 0.0015 (*SE* 0.000016). Using the SNP data set with no missing data, average individual heterozygosity for all 80 individuals was 0.23 (*SD* 0.027), and the average inbreeding coefficient (F_{IS}) was 0.012 (*SD* 0.12). For the 58 unrelated individuals, average heterozygosity was 0.23 (*SD* 0.027), and F_{IS} was 0.019 (*SD* 0.12). Bartlett's test revealed that the variances in observed and expected heterozygosity were not significantly different ($K^2 = 1.68$, $p = .2$). Average F_{IS} was higher on MK than on MT, but the difference was not significant (0.04 and 0.01 respectively, Welch two-sample *t* test $p = .2$). Using the data set with 10% missing data, the probability of two individuals having identical genotypes assuming siblings are present (p_{IDsib}) was 1.54×10^{-199}.

3.4 | Population structure

Both DAPC and STRUCTURE indicated that the most likely number of population clusters was two and the second most likely was

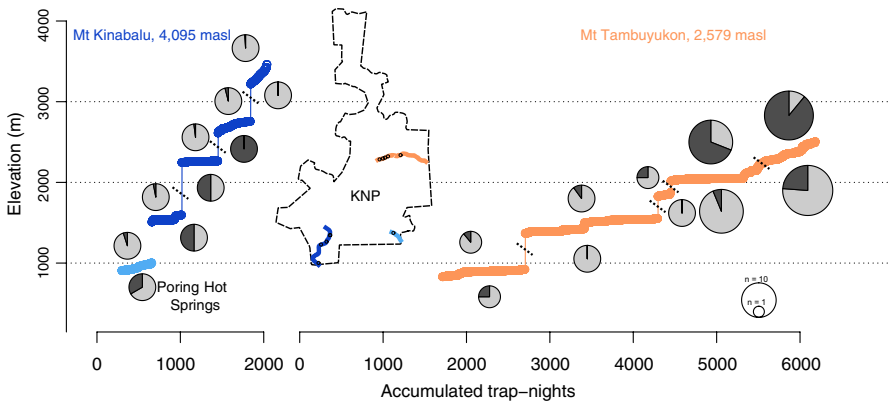

FIGURE 4 Elevations sampled on Mt Kinabalu (900, 1,600, 2,200, 2,700 and 3,200 masl) and Mt Tambuyukon (900, 1,300, 1,600, 2,000 and 2,400 masl) with the distribution of mitochondrial haplogroups per elevation shown below each transect line and SNP clusters above. Colours of each transect line correspond to localities on the inset map (dark blue, MK; light blue, Poring Hot Spring MK; orange, MT). Mitogenome pie charts indicate, for each elevation, the number of treeshrews sampled with a haplotype from mitochondrial haplogroup 1 (light grey) and 2 (dark grey). SNP pie charts indicate for each elevation the proportion of ancestry assigned to cluster 1 (light grey) and cluster 2 (dark grey) by STRUCTURE with $K = 2$, which was determined by the Evanno method to be the most likely number of clusters. The area of each circle is proportional the number of individuals sampled at each elevation

three, as determined by BIC and the Δ*K* method, respectively. The Δ*K* method is biased toward *K* = 2 (Campana et al., 2011; Janes et al., 2017) and simulation studies have shown that the mean probability (MeanLn*P*(*K*)) output from STRUCTURE performs better in scenarios with high gene flow and low F_{ST} (Latch et al., 2006). Because *K* = 3 produced the highest MeanLn*P*(*K*) in STRUCTURE (Table S4a), we consider this a relevant model and show the proportion of individual membership in each cluster as defined by each of the two analyses for both *K* = 2 and *K* = 3 (Figure 5). Results with higher *K* values are shown in Figure S4. We also ran STRUCTURE separately for individuals caught on MK and MT, with settings described above except we ran simulations for *K* = 1–5. We found no evidence of structure among MK individuals; MT individuals were divided into two clusters—one with individuals ≥2,000 masl and one with individuals <2,000 masl, with individuals of mixed ancestry at 2,000 masl (Table S4b,c).

Cluster membership is mostly concordant between DAPC and STRUCTURE, except STRUCTURE assigned mixed ancestry to many individuals while DAPC did not. This is not unexpected as previous studies have shown that DAPC may underestimate admixture (Frosch et al., 2014) while STRUCTURE is more accurate at assigning mixed ancestry (Bohling et al., 2013). When *K* = 2, individuals at 2,000 and 2,400 masl on MT form a separate cluster from low-elevation MT + MK (Figures 4 and 5), with mixed ancestry individuals at 2,000 masl on MT. This shows that the most prominent population subdivision does not separate the two mountains or high and low elevations on MK as we predicted; rather, high-elevation MT is distinct. For *K* = 3, the divisions are between high-elevation MT, low-elevation MT, and MK, with individuals at Poring Hot Spring on the eastern slope of MK (900 masl) and 2,000 masl on MT assigned mixed ancestry (Figure 5). This suggests that no significant substructure exists among MK individuals despite the greater elevational range on this mountain, and that gene flow occurs between MK and MT.

The PCA shows a similar pattern. PC1 (7% variation explained) separates the two mountains, with overlap among individuals at 900 masl. PC2 (4% variation explained) partially separates individuals by elevation, with lower elevation individuals at the midline and right of centre, and high-elevation individuals on the left (Figure 6). The "horseshoe" shape of the plot is typical in isolation-by-distance (IBD) scenarios where genetic similarity decays with geographical distance (Novembre & Stephens, 2008). Because of the spatial pattern evident in our PCA, we ran a spatial PCA (sPCA, Jombart, 2008), which explicitly incorporates spatial autocorrelation between samples and allows for the visualization of genetic structure in space. The results showed the greatest differentiation between high-elevation MT and MK, with weaker, intermediate differentiation separating individuals at low-elevation MT and Poring Hot Springs (Figure S5).

With *K* = 2, after removing individuals that could not be assigned to a STRUCTURE cluster (cutoff q_k value < 0.6), F_{ST} is 0.05 (p = .0001). The AMOVA showed that most variation (95%) is partitioned within

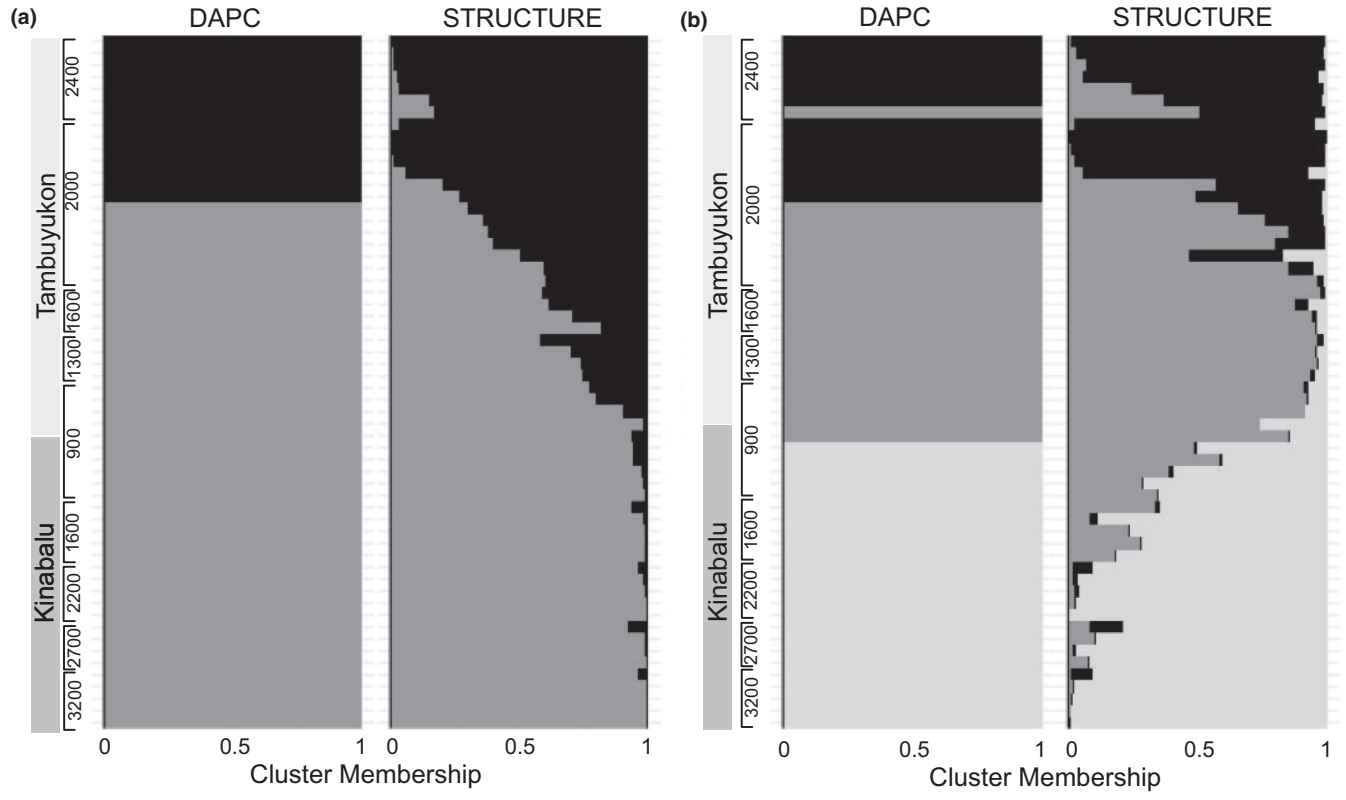

FIGURE 5 Cluster membership according to DAPC and STRUCTURE for (a) *K* = 2 and (b) *K* = 3. For each analysis, *K* = 2 was the best-fitting number of clusters, followed by *K* = 3. Each horizontal line represents a single individual with shading showing how much of each's ancestry can be attributed to each cluster. Individuals are arranged from high-elevation Mt Tambuyukon to low-elevation Mt Tambuyukon followed by low-elevation Mt Kinabalu to high-elevation Mt Kinabalu. Elevations and mountains are labelled on the *y*-axis

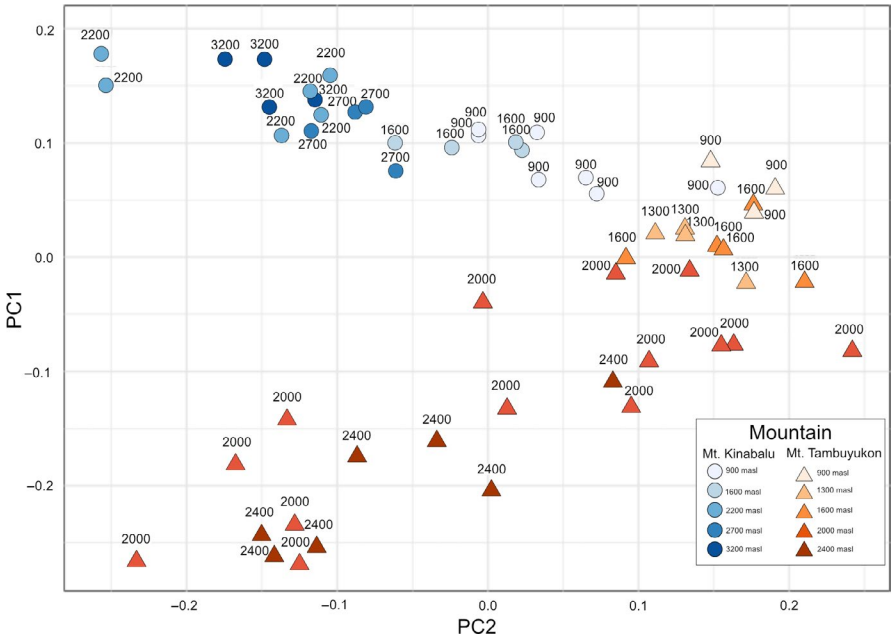

FIGURE 6 Principal components analysis plot with individuals caught on Mt Kinabalu shown in blue circles and Mt Tambuyukon in orange triangles. Individuals sampled at lower elevations are shaded with light colours and high elevation with dark, and each point is labelled with the sampling location elevation. PC1 explains 7% of the variance and PC2 explains 4%

clusters and only 5% between them. With $K = 3$, removing individuals with q_k values <0.6, F_{ST} between MK and low-elevation MT was 0.035 ($p = .001$), between MK and high-elevation MT $F_{ST} = 0.092$ ($p = .0001$), and between low-elevation MT and high-elevation MT $F_{ST} = 0.065$ ($p = .0005$) (Table 2a,b). The AMOVA showed that 94% of the variation is distributed within clusters, and 6% among them.

Including data for all 80 individuals, the Mantel test revealed a significant, positive correlation between genotypic distance and geographical distance ($r = 0.287$, $p = .0001$). Including only the 58 unrelated individuals, the correlation was weaker but statistically significant ($r = 0.05$, $p < .0001$). The correlogram showed significant positive autocorrelation between individuals at distances of 200 m and less ($r = 0.091$, p r-rand ≥ p r-data = 0.0001) and between 200 m and 1 km ($r = 0.036$, p r-rand ≥ p r-data = 0.0001); autocorrelation was no longer significant at 2 km ($r = -0.001$, p r-rand ≥ p r-data = 0.598). At subsequent distance classes (5, 10, 15 and 18 km), individuals have greater genetic distance than expected at random (p r-rand ≤ r-data = 0.009, 0.0001, 0.0001 and 0.0001, respectively; Figure S6). The average geographical distance between pairs of first-order relatives (e.g., parent–offspring or sibling pairs) was 162.5 m, second-order relatives (e.g., half siblings or grandparents–grand-offspring pairs) was 1.2 km, third-order relatives was 4.8 km, and between distant or "unrelated" individuals was 12 km (Table 1); this suggests that in a single generation, individuals on average are unlikely to disperse beyond 162.5 m. Differences between first and third, first and distant, second and distant, and third and distant relatives were significant ($p < .05$).

3.5 | Population and migration models

Model 4 (Figure 2) was the best fit model as determined by Bayes Factors in the MIGRATE-N analysis, followed by Model 5 (Table S5); this was consistent across both runs of the program with alternative phasing. Model 4 divided the population into three groups: high-elevation MT, low-elevation MT, and MK, with high rates of

TABLE 2 Effective population sizes and pairwise F_{ST} of population clusters with (a) $K = 3$ and (b) $K = 2$

	MK	MT < 2,000masl	MT> 2,000masl
(a) $K = 3$			
MK ($n = 22$)	125 (105–152)	0.00120	0.00010
MT < 2,000 masl ($n = 19$)	0.035	202 (157–282)	0.00050
MT> 2,000 masl ($n = 11$)	0.092	0.065	48 (40–59)
	MK + MT < 2,000 masl		MT> 2,000 masl
(b) $K = 2$			
MK + MT < 2,000 masl ($n = 36$)	180 (160–205)		0.0001
MT> 2,000 masl ($n = 18$)	0.050		57 (52–63)

Note: MK, Mount Kinabalu; MT, Mount Tambuyukon. N_e estimates are on the diagonal with 95% confidence interval in parentheses; F_{ST} estimates are below the diagonal, with associated p-values above the diagonal.

bidirectional migration between all pairs (Table S6). Model 5 divided the population into high-elevation MT and low-elevation MT + MK with bidirectional migration (Figure 2). Across models, the mean migration rate from high-elevation MT to MK was greater than from MK to MT (1.3–19×, Table S6).

The results from NEESTIMATOR suggest a larger effective population size on MT (<2,000 masl + ≥2,000 masl) than MK despite less available habitat on MT (250 versus 125 breeding founders, respectively; Table 2 and Supporting Information).

4 | DISCUSSION

4.1 | Levels of gene flow across elevations

Our results are not consistent with Janzen's hypothesis (Janzen, 1967), which predicts narrow elevational distribution and restricted gene flow across elevational gradients in tropical montane species (Ghalambor et al., 2006). We report evidence of high gene flow between MK and MT as well as between low and high elevations on both peaks, indicating that neither the lowland habitat connecting the two peaks, nor the steep elevational gradient across which mountain treeshrews occur on each peak, has significantly limited effective dispersal.

The KNP mountain treeshrew population is best described as comprising two or three clusters, but the primary subdivision does not correspond to the two peaks or separate high- and low-elevation MK as predicted. Rather, the summit region of MT was consistently recovered as distinct in both STRUCTURE and DAPC (Figure 5a). When dividing the population into three clusters, low-elevation individuals at Poring Hot Springs on the eastern slope of MK show mixed ancestry with low-elevation MT (Figure 5b). Additionally, the MIGRATE-N analysis supports the division of individuals into three population clusters (high-elevation MT, low-elevation MT, and MK), with high migration rates between all pairs (Figure 2; Table S6). If gene flow were restricted due to limited elevational dispersal or selection against cross-elevation migrants, we would expect to find greater genetic differentiation on MK because of the broader elevational range and associated diversity of environmental factors on this slope compared to MT. However, the summit of MT was consistently recovered as the most distinct population cluster while individuals caught along the entire elevational gradient on MK form a single cluster (Figures 4 and 5). This suggests that elevation and covarying environmental conditions are not the primary variables influencing mountain treeshrew genetic structure in KNP.

The first prediction of Janzen's (1967) hypothesis, that topical montane species tend to have narrower elevational ranges than those in the temperate zone, has been shown to apply across taxonomic groups including endotherms such as birds (Ghalambor et al., 2006) and bats (McCain, 2009). However, McCain (2009) found that in rodents there was either no relationship between elevational range and latitude or range size increased with decreasing latitude. This finding could be explained by the presence of cryptic species pairs or genetic differentiation separating low- and high-elevation populations. Supporting this hypothesis, some studies of small mammals in Southeast Asia have found strong, cryptic genetic differentiation across elevations, such as in squirrels (den Hinckley et al., 2020; den Tex et al., 2010), shrews (Eldridge et al., 2018) and mice (Heaney et al., 2011; Justiniano et al., 2015). However, McCain (2009) hypothesized that rodents may cope with the lower temperatures associated with increasing altitude through behavioural adaptations. Our finding of high gene flow across a broad elevational extent in mountain treeshrews is not inconsistent with McCain's hypothesis. In addition, Hinckley et al. (in review) found that mountain treeshrews exhibit ecophenotypic changes associated with elevation, including significantly smaller ears and tails and denser hair at higher elevations; these patterns were consistent on both MT and MK. Hinckley et al. suggest that these phenotypic changes, in combination with behaviours including diurnal activity patterns and nesting, may allow the species to persist across broad environmental conditions, which is rare among small mammals in this landscape (Camacho-Sanchez et al., 2019; Hinckley et al., in review; Nor, 2001). Further research is necessary to determine whether the phenotypic changes observed in mountain treeshrews in KNP are due to phenotypic plasticity, adaptive differentiation despite gene flow or a combination of these factors.

4.2 | Population genetic structure shaped by IBD and historical dynamics

The population genetic pattern observed is partly consistent with IBD, as evidenced by (i) the small, but significant, positive correlation between pairwise geographical distance and genetic distance, (ii) spatial autocorrelation between samples drops off at a distance of 2 km (Figure S6), and (iii) pairwise F_{ST} between the nonadjacent MT summit and MK clusters is greater than the value between neighbouring clusters (Table 2a). High gene flow rates between adjacent demes across the landscape, with relatively short dispersal distances as suggested by the correlogram (Figure S6) and ANOVA (Table 1), could have generated the clinal pattern we observe (Figure 5); however, this does not explain the distinctiveness of the summit MT cluster. The Euclidean distance between the lowest and highest sampled points on MK (~13.5 km) is greater than the distance between the lowest and highest sampling points on MT (~4.5 km), yet there is more population genetic differentiation on MT. This indicates that the structure we observe is not due to IBD or isolation-by-elevation alone, and that genetic similarity decays with geographical distance at unequal rates in this landscape (Figure S7a).

Historical population dynamics probably contributed to the observed population genetic structure. Without data from other Bornean localities, it is difficult to determine what process(es) generated the pattern. However, we suggest a plausible scenario given known information about the relative ages of MT and MK and the degree of

divergence between the mountain treeshrew and its sister species. MT reached its current elevation earlier (~11–7 Ma) than MK (~1 Ma; Collenette, 1964; Hall, 1998; Liew et al., 2010). This suggests that MT was available for colonization prior to the split of mountain treeshrews from ruddy treeshrews ~4 Ma (Roberts et al., 2011). If mountain treeshrews were resident on MT prior to a second colonization event, this could explain the signature of two population clusters. We find higher-than-average genetic diversity among individuals at high-elevation MT despite its smaller habitat area (Figure 1a; Figure S7b), which is consistent with our hypothesis that this region maintained a relatively stable, or recently reduced, effective population size over time relative to MK. The lower rate of gene flow upslope to high-elevation MT relative to gene flow towards MK that we observed in the MIGRATE-N analysis (Table S6) may have preserved the signature of this cluster. It is not clear what factors may be limiting upslope gene flow, but one hypothesis is that it is related to a significant shift in the plant community that occurs between 1,450 masl and the summit (van der Ent et al., 2018). Supporting this hypothesis, trapping success of mountain treeshrews and other small mammals is low from 1,500 to 1,800 masl, and increases above 2,000 masl (Camacho-Sanchez et al., 2019). In addition, Hinckley et al. (in review) show differences in musculature related to mastication across elevations, and suggest that these differences may be due to changes in the plant community (i.e., there are fewer fruiting trees at high elevations) and a larger proportion of invertebrates such as beetles in the mountain treeshrew diet.

By contrast, the lack of differentiation across MK could have been influenced by an upslope shift at the mountain treeshrew's upper elevational limit enabled by climate warming and upslope shifts in montane forest since the Last Glacial Maximum (LGM; Cannon et al., 2009; Hall et al., 2009). Upslope shifts in montane forest during this period of warming could have enabled range expansion at high elevations, in addition to range contraction at low elevations. Mountain treeshrews on MT probably did not experience a concurrent upslope range shift because MT has a much lower summit which, unlike the summit of MK, was never covered in ice (Hall et al., 2009). The lack of a population expansion signature in the mountain treeshrew mitogenome data could be explained by unrestricted gene flow between adjacent areas during expansion (Pierce et al., 2017). As predicted for a recent expansion, we find lower-than-average genetic diversity among high-elevation MK individuals (≥1,600 masl) in our SNP data using estimated effective migration surface modelling (Petkova et al., 2016) to visualize genetic diversity on the landscape (Figure S7b).

4.3 | Mito-nuclear discordance

The population genetic pattern inferred from our mitogenome data is discordant with the nuclear SNP data set, although it is not inconsistent with a scenario of two colonization events to KNP. Phylogenetic analyses revealed two divergent mitochondrial lineages within mountain treeshrews; both lineages are found on both mountains, but haplogroups 1 and 2 are equally represented on MK while haplogroup 1 is more frequent on MT (Figures 3 and 4). As mentioned above, MT provided montane habitat earlier than MK. If KNP were colonized a second time by mountain treeshrews from the Crocker Range, this would explain the presence of two sympatric, divergent lineages within Kinabalu Park. The greater frequency of haplogroup 2 on MK could be explained by the closer geographical proximity of MK to the Crocker Range (Figure S8), combined with male-biased dispersal limiting the movement of haplogroup 2 from MK to MT. There is no information on dispersal differences between sexes in mountain treeshrews. Male-biased dispersal is common among mammals (Greenwood, 1980), but female-biased dispersal has been documented in the large treeshrew (Munshi-South, 2008). Lack of recombination in the mitochondrial genome would have retained the signature of divergence between the two haplogroups whereas recombination in nuclear SNPs would result in genetic admixture between the two groups.

This pattern could also be the result of a single colonization event of two sympatric lineages that diverged elsewhere in Borneo, for example due to isolation in interglacial refugia and mixing during glacial maxima when montane forest was at its maximum extent (Cannon et al., 2009; den Tex et al., 2010). However, this scenario implies that the colonization of KNP by mountain treeshrews would have occurred after the divergence between the two lineages ~450,000 years ago, which is relatively recent compared to the age of MT (at least 7 million years) and the age of the species (~4 million years). Additionally, multiple colonization events to MK have been inferred in other taxa, including plants in the genus *Rhododendron* (Merckx et al., 2015).

Gawin et al. (2014) documented a similar pattern in mountain blackeyes (*Chlorocharis emiliae*) in Borneo; they found two divergent mitochondrial haplogroups on MK, with one lineage sister to a lineage found on Mt Trus Madi, a mountain south of MK within the Crocker Range (Figure S8). The pattern inferred from SNP data in a subsequent study was not concordant, with a single lineage found on MK (Manthey et al., 2017). This similar pattern may indicate a common colonization history between mountain blackeyes and mountain treeshrews. Future studies should include broader geographical sampling of mountain treeshrews, including individuals from across the Crocker Range, to test the hypothesis of multiple colonization events and to determine the phylogeographical history of this species in Borneo.

4.4 | UCEs for fine-scale population genomics

Here, we show that sequence capture of ~5,000 UCEs yielded two highly informative data sets (i.e., SNPs and phased pseudohaplotype sequences) suitable for population genomics on a fine spatial scale. These data sets resolved patterns of fine-scale, weak population structure in mountain treeshrews within KNP, an area of ~754 km^2. The SNP data set provided sufficient statistical power to identify individuals with high probability ($p_{\mathrm{IDsib}} = 1.54 \times 10^{-199}$), to identify putative family groups using pairwise kinship estimates, and to reveal patterns of population structure with low levels of differentiation (Figure 5; Table 2).

Although our results suggest that UCE loci may be sufficiently variable for population genomic studies, more research is necessary to determine the substitution rate of these markers and its effect on demographic parameters derived from the site-frequency spectrum (Winker et al., 2018). Previous studies have suggested that the highly conserved cores of UCE loci are subject to strong purifying selection. While the strength of selection decreases and the substitution rate increases with distance from the core (Katzman et al., 2007), UCE-flanking regions may have lower diversity than other genomic markers, leading to an excess of rare alleles (Cvijović et al., 2018).

UCEs are valuable for studying species like the mountain treeshrew for which few genomic resources are available. RAD-sequencing (RAD-seq) methods also do not require reference genomes and can generate an order of magnitude more loci than UCE-based methods; this dense genomic sampling enables investigation of both neutral and adaptive differentiation (Hohenlohe et al., 2010), which is particularly important for defining conservation units (Funk et al., 2012). However, for inferences regarding population structure and gene flow, it has been shown that fewer than 100 informative SNP loci are sufficient (von Thaden et al., 2020) and here we analysed 1,794 independent SNPs. Additionally, the average heterozygosity of our UCE-derived SNPs is 0.23, similar to that reported in RAD-seq studies of other small mammal populations, including mice of the genera *Apodemus* (0.28; Cerezo et al., 2020) and *Peromyscus* (0.148–0.239; Garcia-Elfring et al., 2019).

In summary, although more research is needed into the substitution rate of UCE loci and its effect on demographic inferences, our results show that UCE capture methods can be used for fine-scale population genomics, providing an additional tool for studying nongenome-enabled species. UCE capture produces data with similar information content and has several benefits over RAD-seq, including: (i) enabling the direct comparison of inferences drawn from the same set of loci across species, allowing conclusions to be drawn about the effects of historical processes on diverse taxa (Lim et al., 2020); (ii) offering repeatability such that studies can compare inferences for the same species across time and geographical regions (Harvey et al., 2016); and (iii) enabling the use of low-quality DNA, including DNA derived from historical museum specimens (Hawkins et al., 2016; Lim & Braun, 2016; Lim et al., 2020; Tsai et al., 2019).

4.5 | Conservation implications

As a tropical montane species, the mountain treeshrew may be impacted by GCC, which is predicted to shift montane communities in KNP upslope ~490 m by the year 2,100 (Camacho-Sanchez et al., 2018; Still et al., 1999) assuming mild Intergovernmental Panel on Climate Change scenarios (IPCC 2013, www.ipcc.ch/report/ar5/wg1/). Although the factors that limit the mountain treeshrew at its lower elevational boundary are unknown, assuming that the species tracks the predicted 490-m upslope shift—whether because of climatic limitations or ecological interactions with lowland species expanding upslope—we predict that it will experience range contraction. The species already occupies the upper elevational limits within KNP, so an upslope shift in the lower bound of its distribution could not be countered with expansion at its upper limit. The lack of strong population structure across elevations means that upslope dispersal of lower elevation mountain treeshrews on MK will probably not increase extinction risk by introducing maladaptive genetic diversity (Weiss-Lehman & Shaw, 2019). However, reduction in available habitat could make the species vulnerable.

We also predict that in this scenario of upslope habitat shifts, mountain treeshrews would maintain connectivity between MK and MT. However, the Crocker Range has few peaks above 1,400 masl, and connectivity between KNP and the rest of the Crocker Range could be severed (Figure S8). This highlights the importance of KNP as a future refugium for montane species, as it contains the highest peak in the region and the greatest high-elevation forested area. Conservation efforts should focus on protecting forest habitat at 900 masl outside the park to facilitate gene flow and preserve genetic diversity.

ACKNOWLEDGEMENTS

L. Olson, C. Thompson and UMMZ provided Tupaia splendidula DNA extracts. S. Lindley and the FDA donated a MiSeq sequencing kit. T. Giarla shared his SNP calling scripts. S. Castañeda Rico, M-E. Ochirbat, M. Venkatraman, N. R. McInerney, A. M. Kearns and A. W. Kaganer provided helpful comments on the manuscript. K. Helgen and R. Fleischer provided logistical support. Chien Lee provided the mountain treeshrew photograph. This work was funded by the Spanish Government (CGL2010-21524, CGL2017-86068-P), the Smithsonian Institution (Building the Framework of Biodiversity Science: Next Generation Phylogenomics Smithsonian Grand Challenges Awards 2012–2014), the National Science Foundation (1547168, 1717498), and the Department of Biology at George Mason University. Logistical support was provided by Laboratorio de Sistemas de Información Geográfica y Teledetección de la Estación Biológica de Doñana and Doñana ICTS-RBD. We also wish to thank three anonymous reviewers for comments that greatly improved the quality of the manuscript.

AUTHOR CONTRIBUTIONS

M.T.R.H., M.C.S. and J.A.L. organized fieldwork; M.T.R.H. and M.C.S. conducted fieldwork; M.T.R.H., J.A.L., J.E.M. and L.D.P. designed the study; J.A.L., J.E.M. and L.L.R. provided resources for the study; M.T.R.H. and L.D.P. did laboratory work; L.D.P. wrote the manuscript and performed UCE analyses; M.T.R.H. performed phylogenetic analyses; M.C.S. contributed figures; T.R.W., H.C.L. and M.G.C. assisted in bioinformatics; M.G.C. and J.A.W. developed vcf2aln; all authors participated in revisions and acceptance of the final version of the manuscript.

DATA AVAILABILITY STATEMENT

DNA sequences: GenBank accessions MT423905–MT423940 and MT442045–MT442052; NCBI SRA PRJNA629376.

MIGRATE-N input file on FigShare, https://doi.org/10.25573/data.12168225.

ORCID

Lillian D. Parker https://orcid.org/0000-0003-3370-9473
Miguel Camacho-Sanchez https://orcid.org/0000-0002-6385-7963
Michael G. Campana https://orcid.org/0000-0003-0461-6462
Jennifer A. Leonard https://orcid.org/0000-0003-0291-7819

REFERENCES

Andermann, T., Fernandes, A. M., Olsson, U., Töpel, M., Pfeil, B., Oxelman, B., Aleixo, A., Faircloth, B. C., & Antonelli, A. (2018). Allele phasing greatly improves the phylogenetic utility of ultraconserved elements. *Systematic Biology*, *68*(1), 32–46. https://doi.org/10.1093/sysbio/syy039

Beerli, P. (2005). Comparison of Bayesian and maximum-likelihood inference of population genetic parameters. *Bioinformatics*, *22*(3), 341–345. https://doi.org/10.1093/bioinformatics/bti803

Beerli, P., & Palczewski, M. (2010). Unified framework to evaluate panmixia and migration direction among multiple sampling locations. *Genetics*, *185*(1), 313–326. https://doi.org/10.1534/genetics.109.112532

Bertrand, J. A. M., Bourgeois, Y. X. C., Delahaie, B., Duval, T., García-Jiménez, R., Cornuault, J., Heeb, P., Milá, B., Pujol, B., & Thébaud, C. (2014). Extremely reduced dispersal and gene flow in an island bird. *Heredity*, *112*(2), 190–196. https://doi.org/10.1038/hdy.2013.91

Bohling, J. H., Adams, J. R., & Waits, L. P. (2013). Evaluating the ability of Bayesian clustering methods to detect hybridization and introgression using an empirical red wolf data set. *Molecular Ecology*, *22*(1), 74–86. https://doi.org/10.1111/mec.12109

Bolger, A. M., Lohse, M., & Usadel, B. (2014). Trimmomatic: A flexible trimmer for Illumina sequence data. *Bioinformatics*, *30*(15), 2114–2120. https://doi.org/10.1093/bioinformatics/btu170

Bouckaert, R., Heled, J., Kühnert, D., Vaughan, T., Wu, C.-H., Xie, D., Suchard, M. A., Rambaut, A., & Drummond, A. J. (2014). BEAST 2: A software platform for Bayesian evolutionary analysis. *PLoS Computational Biology*, *10*(4), e1003537. https://doi.org/10.1371/journal.pcbi.1003537

Branch, C. L., Jahner, J. P., Kozlovsky, D. Y., Parchman, T. L., & Pravosudov, V. V. (2017). Absence of population structure across elevational gradients despite large phenotypic variation in mountain chickadees (*Poecile gambeli*). *Royal Society Open Science*, *4*(3), 170057. https://doi.org/10.1098/rsos.170057

Camacho-Sanchez, M., Hawkins, M. T. R., Tuh Yit Yu, F., Maldonado, J. E., & Leonard, J. A. (2019). Endemism and diversity of small mammals along two neighboring Bornean mountains. *PeerJ*, *7*, e7858. https://doi.org/10.7717/peerj.7858

Camacho-Sanchez, M., Quintanilla, I., Hawkins, M. T. R., Tuh Yit Yu, F., Wells, K., Maldonado, J. E., & Leonard, J. A. (2018). Interglacial refugia on tropical mountains: Novel insights from the summit rat (*Rattus baluensis*), a Borneo mountain endemic. *Diversity and Distributions*, *24*, 1252–1266. https://doi.org/10.1111/ddi.12761

Campana, M. G., Hunt, H. V., Jones, H., & White, J. (2011). CorrSieve: Software for summarizing and evaluating structure output. *Molecular Ecology Resources*, *11*(2), 349–352. https://doi.org/10.1111/j.1755-0998.2010.02917.x

Cannon, C. H., Morley, R. J., & Bush, A. B. G. (2009). The current refugial rainforests of Sundaland are unrepresentative of their biogeographic past and highly vulnerable to disturbance. *Proceedings of the National Academy of Sciences of the United States of America*, *106*(27), 11188–11193. https://doi.org/10.1073/pnas.0809865106

Castillo Vardaro, J. A., Epps, C. W., Frable, B. W., & Ray, C. (2018). Identification of a contact zone and hybridization for two subspecies of the American pika (*Ochotona princeps*) within a single protected area. *PLoS One*, *13*(7), e0199032. https://doi.org/10.1371/journal.pone.0199032

Castresana, J. (2000). Selection of conserved blocks from multiple alignments for their use in phylogenetic analysis. *Molecular Biology and Evolution*, *17*(4), 540–552. https://doi.org/10.1093/oxfordjournals.molbev.a026334

Cerezo, M. L. M., Kucka, M., Zub, K., Chan, Y. F., & Bryk, J. (2020). Population structure of *Apodemus flavicollis* and comparison to *Apodemus sylvaticus* in northern Poland based on RAD-seq. *BMC Genomics*, *21*(1), 241. https://doi.org/10.1186/s12864-020-6603-3

Chen, B., Cole, J. W., & Grond-Ginsbach, C. (2017). Departure from Hardy Weinberg equilibrium and genotyping error. *Frontiers in Genetics*, *8*, 167. https://doi.org/10.3389/fgene.2017.00167

Cheviron, Z. A., & Brumfield, R. T. (2009). Migration-selection balance and local adaptation of mitochondrial haplotypes in rufous-collared sparrows (*Zonotrichia capensis*) along an elevational gradient. *Evolution*, *63*(6), 1593–1605. https://doi.org/10.1111/j.1558-5646.2009.00644.x

Chin, L., Moran, J. A., & Clarke, C. (2010). Trap geometry in three giant montane pitcher plant species from Borneo is a function of tree shrew body size. *New Phytologist*, *186*(2), 461–470. https://doi.org/10.1111/j.1469-8137.2009.03166.x

Clarke, C. M., Bauer, U., Lee, C. C., Tuen, A. A., Rembold, K., & Moran, J. A. (2009). Tree shrew lavatories: A novel nitrogen sequestration strategy in a tropical pitcher plant. *Biology Letters*, *5*(5), 632–635. https://doi.org/10.1098/rsbl.2009.0311

Collenette, P. (1964). A short account of the geology and geological history of Mt. Kinabalu. *Proceedings of the Royal Society of London Series B, Biological Sciences*, *161*, 56–63.

Combs, M., Puckett, E. E., Richardson, J., Mims, D., & Munshi-South, J. (2017). Spatial population genomics of the brown rat (*Rattus norvegicus*) in New York City. *Molecular Ecology*, *27*(1), 83–98. https://doi.org/10.1111/mec.14437

Conomos, M. P., Reiner, A. P., Weir, B. S., & Thornton, T. A. (2016). Model-free estimation of recent genetic relatedness. *The American Journal of Human Genetics*, *98*(1), 127–148. https://doi.org/10.1016/j.ajhg.2015.11.022

Cvijović, I., Good, B. H., & Desai, M. M. (2018). The effect of strong purifying selection on genetic diversity. *Genetics*, *209*(4), 1235. https://doi.org/10.1534/genetics.118.301058

Danecek, P., Auton, A., Abecasis, G., Albers, C. A., Banks, E., DePristo, M. A., Handsaker, R. E., Lunter, G., Marth, G. T., Sherry, S. T., McVean, G., & Durbin, R.; 1000 Genomes Project Analysis Group. (2011). The variant call format and VCFtools. *Bioinformatics*, *27*(15), 2156–2158. https://doi.org/10.1093/bioinformatics/btr330

den Tex, R. J., Thorington, R., Maldonado, J. E., & Leonard, J. A. (2010). Speciation dynamics in the *SE* Asian tropics: Putting a time perspective on the phylogeny and biogeography of Sundaland tree squirrels, Sundasciurus. *Molecular Phylogenetics and Evolution*, *55*(2), 711–720. https://doi.org/10.1016/j.ympev.2009.12.023

Do, C., Waples, R. S., Peel, D., Macbeth, G. M., Tillett, B. J., & Ovenden, J. R. (2014). NeEstimator v2: Re-implementation of software for the estimation of contemporary effective population size (Ne) from genetic data. *Molecular Ecology Resources*, *14*(1), 209–214. https://doi.org/10.1111/1755-0998.12157

Dray, S., & Dufour, A. B. (2007). The Ade4 package: Implementing the duality diagram for ecologists. *Journal of Statistical Software*, *1*(4), 1–20. https://doi.org/10.18637/jss.v022.i04

Drummond, A. J., & Rambaut, A. (2007). BEAST: Bayesian evolutionary analysis by sampling trees. *BMC Evolutionary Biology*, *7*(1), 214. https://doi.org/10.1186/1471-2148-7-214

DuBay, S. G., & Witt, C. C. (2014). Differential high-altitude adaptation and restricted gene flow across a mid-elevation hybrid zone in Andean tit-tyrant flycatchers. *Molecular Ecology*, *23*(14), 3551–3565. https://doi.org/10.1111/mec.12836

Earl, D. A., & vonHoldt, B. M. (2012). STRUCTURE HARVESTER: A website and program for visualizing STRUCTURE output and implementing the Evanno method. *Conservation Genetics Resources*, *4*(2), 359–361. https://doi.org/10.1007/s12686-011-9548-7

Eldridge, R. A., Achmadi, A. S., Giarla, T. C., Rowe, K. C., & Esselstyn, J. A. (2018). Geographic isolation and elevational gradients promote diversification in an endemic shrew on Sulawesi. *Molecular Phylogenetics and Evolution*, *118*, 306–317. https://doi.org/10.1016/j.ympev.2017.09.018

Emmons, L. H. (2000). *Tupai: A field study of Bornean treeshrews*. University of California Press.

Evanno, G., Regnaut, S., & Goutdet, J. (2005). Detecting the number of clusters of individuals using the software STRUCTURE: A simulation study. *Molecular Ecology*, *14*(8), 2611–2620. https://doi.org/10.1111/j.1365-294X.2005.02553.x

Excoffier, L., & Lischer, H. E. L. (2010). Arlequin suite ver. 3.5: A new series of programs to perform population genetics analyses under Linux and Windows. *Molecular Ecology Resources*, *10*(3), 564–567. https://doi.org/10.1111/j.1755-0998.2010.02847.x

Faircloth, B. C. (2016). PHYLUCE is a software package for the analysis of conserved genomic loci. *Bioinformatics*, *32*(5), 786–788. https://doi.org/10.1093/bioinformatics/btv646

Faircloth, B. C., McCormack, J. E., Crawford, N. G., Harvey, M. G., Brumfield, R. T., & Glenn, T. C. (2012). Ultraconserved elements anchor thousands of genetic markers spanning multiple evolutionary timescales. *Systematic Biology*, *61*(5), 717–726. https://doi.org/10.1093/sysbio/sys004

Falush, D., Stephens, M., & Pritchard, J. K. (2003). Inference of population structure using multilocus genotype data: Linked loci and correlated allele frequencies. *Genetics*, *164*(4), 1567–1587.

Feeley, K. J., Stroud, J. T., & Perez, T. M. (2017). Most 'global' reviews of species' responses to climate change are not truly global. *Diversity and Distributions*, *23*(3), 231–234. https://doi.org/10.1111/ddi.12517

Feijó, A., Wen, Z., Cheng, J., Ge, D., Xia, L., & Yang, Q. (2019). Divergent selection along elevational gradients promotes genetic and phenotypic disparities among small mammal populations. *Ecology and Evolution*, *9*(12), 7080–7095. https://doi.org/10.1002/ece3.5273

Felsenstein, J. (2005). Accuracy of coalescent likelihood estimates: Do we need more sites, more sequences, or more loci? *Molecular Biology and Evolution*, *23*(3), 691–700. https://doi.org/10.1093/molbev/msj079

Frosch, C., Kraus, R. H. S., Angst, C., Allgöwer, R., Michaux, J., Teubner, J., & Nowak, C. (2014). The genetic legacy of multiple beaver reintroductions in central Europe. *PLoS One*, *9*(5), e97619. https://doi.org/10.1371/journal.pone.0097619

Funk, W. C., McKay, J. K., Hohenlohe, P. A., & Allendorf, F. W. (2012). Harnessing genomics for delineating conservation units. *Trends in Ecology & Evolution*, *27*(9), 489–496. https://doi.org/10.1016/j.tree.2012.05.012

Gadek, C. R., Newsome, S. D., Beckman, E. J., Chavez, A. N., Galen, S. C., Bautista, E., & Witt, C. C. (2018). Why are tropical mountain passes 'low' for some species? Genetic and stable-isotope tests for differentiation, migration and expansion in elevational generalist songbirds. *Journal of Animal Ecology*, *87*(3), 741–753. https://doi.org/10.1111/1365-2656.12779

Garcia-Elfring, A., Barrett, R. D. H., & Millien, V. (2019). Genomic signatures of selection along a climatic gradient in the northern range margin of the white-footed mouse (*Peromyscus leucopus*). *Journal of Heredity*, *110*(6), 684–695. https://doi.org/10.1093/jhered/esz045

Gawin, D. F., Rahman, M. A., Ramji, M. F. S., Smith, B. T., Lim, H. C., Moyle, R. G., & Sheldon, F. H. (2014). Patterns of avian diversification in Borneo: The case of the endemic mountain black-eye (*Chlorocharis emiliae*). *The Auk*, *131*(1), 86–99. https://doi.org/10.1642/AUK-13-190.1

Ghalambor, C. K., Huey, R. B., Martin, P. R., Tewksbury, J. J., & Wang, G. (2006). Are mountain passes higher in the tropics? Janzen's hypothesis revisited. *Integrative and Comparative Biology*, *46*(1), 5–17. https://doi.org/10.1093/icb/icj003

Giarla, T. C., & Esselstyn, J. A. (2015). The challenges of resolving a rapid, recent radiation: Empirical and simulated phylogenomics of Philippine shrews. *Systematic Biology*, *64*(5), 727–740. https://doi.org/10.1093/sysbio/syv029

Giarla, T. C., Maher, S. P., Achmadi, A. S., Moore, M. K., Swanson, M. T., Rowe, K. C., & Esselstyn, J. A. (2018). Isolation by marine barriers and climate explain areas of endemism in an island rodent. *Journal of Biogeography*, *45*(9), 2053–2066. https://doi.org/10.1111/jbi.13392

Gilbert, P. S., Wu, J., Simon, M. W., Sinsheimer, J. S., & Alfaro, M. E. (2018). Filtering nucleotide sites by phylogenetic signal to noise ratio increases confidence in the Neoaves phylogeny generated from ultraconserved elements. *Molecular Phylogenetics and Evolution*, *126*, 116–128. https://doi.org/10.1016/j.ympev.2018.03.033

Gill, B. A., Kondratieff, B. C., Casner, K. L., Encalada, A. C., Flecker, A. S., Gannon, D. G., Ghalambor, C. K., Guayasamin, J. M., Poff, N. L., Simmons, M. P., Thomas, S. A., Zamudio, K. R., & Funk, W. C. (2016). Cryptic species diversity reveals biogeographic support for the 'mountain passes are higher in the tropics' hypothesis. *Proceedings of the Royal Society B: Biological Sciences*, *283*(1832), 20160553. https://doi.org/10.1098/rspb.2016.0553

Goldberg, C. S., & Waits, L. P. (2010). Quantification and reduction of bias from sampling larvae to infer population and landscape genetic structure. *Molecular Ecology Resources*, *10*(2), 304–313. https://doi.org/10.1111/j.1755-0998.2009.02755.x

Greenwood, P. J. (1980). Mating systems, philopatry and dispersal in birds and mammals. *Animal Behaviour*, *28*(4), 1140–1162. https://doi.org/10.1016/S0003-3472(80)80103-5

Gueuning, M., Suchan, T., Rutschmann, S., Gattolliat, J.-L., Jamsari, J., Kamil, A. I., Pitteloud, C., Buerki, S., Balke, M., Sartori, M., & Alvarez, N. (2017). Elevation in tropical sky islands as the common driver in structuring genes and communities of freshwater organisms. *Scientific Reports*, *7*(1), 16089. https://doi.org/10.1038/s41598-017-16069-y

Hall, R. (1998). The plate tectonics of Cenozoic *SE* Asia and the distribution of land and sea. In R. Hall, & J. D. Holloway (Eds.), *Biogeography and the geological evolution of SE Asia* (pp. 99–131). Backhuys Publishers.

Hall, R., Cottam, M., Suggate, S., Tongkul, F., Sperber, C., & Batt, G. E. (2009). *The geology of Mount Kinabalu*. Sabah, Malaysia.

Harrison, R. G. (1989). Animal mitochondrial DNA as a genetic marker in population and evolutionary biology. *Trends in Ecology & Evolution*, *4*(1), 6–11. https://doi.org/10.1016/0169-5347(89)90006-2

Harvey, M. G., Smith, B. T., Glenn, T. C., Faircloth, B. C., & Brumfield, R. T. (2016). Sequence capture versus restriction site associated DNA sequencing for shallow systematics. *Systematic Biology*, *65*(5), 910–924. https://doi.org/10.1093/sysbio/syw036

Hawkins, M. T. R., Leonard, J. A., Helgen, K. M., McDonough, M. M., Rockwood, L. L., & Maldonado, J. E. (2016). Evolutionary history of endemic Sulawesi squirrels constructed from UCEs and mitogenomes sequenced from museum specimens. *BMC Evolutionary Biology*, *16*(1), 80. https://doi.org/10.1186/s12862-016-0650-z

Heaney, L. R., Balete, D. S., Rickart, E. A., Alviola, P. A., Duya, M. R. M., Duya, M. V., & Steppan, S. J. (2011). Seven new species and a new subgenus of forest mice (Rodentia: Muridae: Apomys) from Luzon Island. *Fieldiana Life and Earth Sciences*, *2011*(2), 1–60.

Hinckley, A., Hawkins, M. T. R., Achmadi, A. S., Maldonado, J. E., & Leonard, J. A. (2020). Ancient divergence driven by geographic

isolation and ecological adaptation in forest dependent Sundaland tree squirrels. *Frontiers in Ecology and Evolution*, *8*, 208. https://doi.org/10.3389/fevo.2020.00208

Hinckley, A., Sanchez-Donoso, I., Comas, M., Camacho-Sanchez, M., Hasan, N. H., & Leonard, J. A. (in review). Challenging ecogeographical rules: Phenotypic variation in the mountain treeshrew (Tupaia montana) along tropical elevational gradients.

Hohenlohe, P. A., Bassham, S., Etter, P. D., Stiffler, N., Johnson, E. A., & Cresko, W. A. (2010). Population genomics of parallel adaptation in threespine stickleback using sequenced RAD tags. *PLoS Genetics*, *6*(2), e1000862. https://doi.org/10.1371/journal.pgen.1000862

Jakobsson, M., & Rosenberg, N. A. (2007). CLUMPP: A cluster matching and permutation program for dealing with label switching and multimodality in analysis of population structure. *Bioinformatics*, *23*(14), 1801–1806. https://doi.org/10.1093/bioinformatics/btm233

Janes, J. K., Miller, J. M., Dupuis, J. R., Malenfant, R. M., Gorrell, J. C., Cullingham, C. I., & Andrew, R. L. (2017). The K = 2 conundrum. *Molecular Ecology*, *26*(14), 3594–3602. https://doi.org/10.1111/mec.14187

Janzen, D. H. (1967). Why mountain passes are higher in the tropics. *The American Naturalist*, *101*(919), 233–249. https://doi.org/10.1086/282487

Jombart, T. (2008). Adegenet: An R package for the multivariate analysis of genetic markers. *Bioinformatics*, *24*(11), 1403–1405. https://doi.org/10.1093/bioinformatics/btn129

Justiniano, R., Schenk, J. J., Balete, D. S., Rickart, E. A., Esselstyn, J. A., Heaney, L. R., & Steppan, S. J. (2015). Testing diversification models of endemic Philippine forest mice (Apomys) with nuclear phylogenies across elevational gradients reveals repeated colonization of isolated mountain ranges. *Journal of Biogeography*, *42*(1), 51–64.

Katoh, K., Misawa, K., Kuma, K., & Miyata, T. (2002). MAFFT: A novel method for rapid multiple sequence alignment based on fast Fourier transform. *Nucleic Acids Research*, *30*(14), 3059–3066. https://doi.org/10.1093/nar/gkf436

Katzman, S., Kern, A. D., Bejerano, G., Fewell, G., Fulton, L., Wilson, R. K., Salama, S. R., & Haussler, D. (2007). Human genome ultraconserved elements are ultraselected. *Science*, *317*(5840), 915. https://doi.org/10.1126/science.1142430

Khaliq, I., Hof, C., Prinzinger, R., Böhning-Gaese, K., & Pfenninger, M. (2014). Global variation in thermal tolerances and vulnerability of endotherms to climate change. *Proceedings of the Royal Society Biological Sciences*, *281*, 20141097. https://doi.org/10.1098/rspb.2014.1097

Kitayama, K. (1992). An altitudinal transect study of the vegetation on Mount Kinabalu, Borneo. *Vegetatio*, *102*(2), 149–171.

Kumar, S., Stecher, G., & Tamura, K. (2016). MEGA7: Molecular evolutionary genetics analysis version 7.0 for bigger datasets. *Molecular Biology and Evolution*, *33*(7), 1870–1874. https://doi.org/10.1093/molbev/msw054

Lanfear, R., Calcott, B., Ho, S. Y. W., & Guindon, S. (2012). PartitionFinder: Combined selection of partitioning schemes and substitution models for phylogenetic analyses. *Molecular Biology and Evolution*, *29*(6), 1695–1701. https://doi.org/10.1093/molbev/mss020

Latch, E. K., Dharmarajan, G., Glaubitz, J. C., & Rhodes, O. E. (2006). Relative performance of Bayesian clustering software for inferring population substructure and individual assignment at low levels of population differentiation. *Conservation Genetics*, *7*(2), 295–302. https://doi.org/10.1007/s10592-005-9098-1

Leigh, J. W., & Bryant, D. (2015). Popart: Full-feature software for haplotype network construction. *Methods in Ecology and Evolution*, *6*(9), 1110–1116. https://doi.org/10.1111/2041-210X.12410

Lenoir, J., & Svenning, J. C. (2015). Climate-related range shifts – A global multidimensional synthesis and new research directions. *Ecography*, *38*(1), 15–28. https://doi.org/10.1111/ecog.00967

Li, H. (2013). Aligning sequence reads, clone sequences and assembly contigs with BWA-MEM. ArXiv 1303.3997v1.

Li, H., Handsaker, B., Wysoker, A., Fennell, T., Ruan, J., Homer, N., Marth, G., Abecasis, G., & Durbin, R.; 1000 Genome Project Data Processing Subgroup. (2009). The sequence alignment/map format and SAMtools. *Bioinformatics*, *25*(16), 2078–2079. https://doi.org/10.1093/bioinformatics/btp352

Librado, P., & Rozas, J. (2009). DnaSP v5: A software for comprehensive analysis of DNA polymorphism data. *Bioinformatics*, *25*(11), 1451–1452. https://doi.org/10.1093/bioinformatics/btp187

Liew, T. S., Schilthuizen, M., & Bin Lakim, M. (2010). The determinants of land snail diversity along a tropical elevational gradient: Insularity, geometry and niches. *Journal of Biogeography*, *37*(6), 1071–1078. https://doi.org/10.1111/j.1365-2699.2009.02243.x

Lim, H. C., & Braun, M. J. (2016). High-throughput SNP genotyping of historical and modern samples of five bird species via sequence capture of ultraconserved elements. *Molecular Ecology Resources*, *16*(5), 1204–1223. https://doi.org/10.1111/1755-0998.12568

Lim, H. C., Shakya, S. B., Harvey, M. G., Moyle, R. G., Fleischer, R. C., Braun, M. J., & Sheldon, F. H. (2020). Opening the door to greater phylogeographic inference in Southeast Asia: Comparative genomic study of five codistributed rainforest bird species using target capture and historical DNA. *Ecology and Evolution*, *10*, 3222–3247. https://doi.org/10.1002/ece3.5964

Linck, E., Freeman, B. G., & Dumbacher, J. P. (2019). Speciation and gene flow across an elevational gradient in New Guinea kingfishers. BioRxiv, 589044. https://doi.org/10.1101/589044

Manichaikul, A., Mychaleckyj, J. C., Rich, S. S., Daly, K., Sale, M., & Chen, W. M. (2010). Robust relationship inference in genome-wide association studies. *Bioinformatics*, *26*(22), 2867–2873. https://doi.org/10.1093/bioinformatics/btq559

Manthey, J. D., Moyle, R. G., Gawin, D. F., Rahman, M. A., Ramji, M. F. S., & Sheldon, F. H. (2017). Genomic phylogeography of the endemic mountain black-eye of Borneo (*Chlorocharis emiliae*): Montane and lowland populations differ in patterns of Pleistocene diversification. *Journal of Biogeography*, *44*(10), 2272–2283. https://doi.org/10.1111/jbi.13028

Mason, N. A., Olvera-Vital, A., Lovette, I. J., & Navarro-Sigüenza, A. G. (2018). Hidden endemism, deep polyphyly, and repeated dispersal across the Isthmus of Tehuantepec: Diversification of the white-collared seedeater complex (Thraupidae: *Sporophila torqueola*). *Ecology and Evolution*, *8*(3), 1867–1881. https://doi.org/10.1002/ece3.3799

McCain, C. M. (2009). Vertebrate range sizes indicate that mountains may be 'higher' in the tropics. *Ecology Letters*, *12*(6), 550–560. https://doi.org/10.1111/j.1461-0248.2009.01308.x

McKenna, A., Hanna, M., Banks, E., Sivachenko, A., Cibulskis, K., Kernytsky, A., Garimella, K., Altshuler, D., Gabriel, S., Daly, M., & DePristo, M. A. (2010). The genome analysis toolkit: A MapReduce framework for analyzing next-generation DNA sequencing data. *Genome Research*, *20*(9), 1297–1303. https://doi.org/10.1101/gr.107524.110

McKinney, G. J., Waples, R. K., Seeb, L. W., & Seeb, J. E. (2017). Paralogs are revealed by proportion of heterozygotes and deviations in read ratios in genotyping-by-sequencing data from natural populations. *Molecular Ecology Resources*, *17*(4), 656–669. https://doi.org/10.1111/1755-0998.12613

Merckx, V. S. F. T., Hendriks, K. P., Beentjes, K. K., Mennes, C. B., Becking, L. E., Peijnenburg, K. T. C. A., Afendy, A., Arumugam, N., de Boer, H., Biun, A., Buang, M. M., Chen, P.-P., Chung, A. Y. C., Dow, R., Feijen, F. A. A., Feijen, H., Soest, C.-V., Geml, J., Geurts, R., & Schilthuizen, M. (2015). Evolution of endemism on a young tropical mountain. *Nature*, *524*(7565), 347–350. https://doi.org/10.1038/nature14949

Moritz, C. (1994). Defining 'evolutionarily significant units' for conservation. *Trends in Ecology & Evolution*, *9*(10), 373–375. https://doi.org/10.1016/0169-5347(94)90057-4

Muenchow, J., Dieker, P., Kluge, J., Kessler, M., & von Wehrden, H. (2018). A review of ecological gradient research in the tropics:

Identifying research gaps, future directions, and conservation priorities. *Biodiversity and Conservation*, *27*(2), 273–285. https://doi.org/10.1007/s10531-017-1465-y

Munshi-South, J. (2008). Female-biased dispersal and gene flow in a behaviorally monogamous mammal, the large treeshrew (*Tupaia tana*). *PLoS One*, *3*(9), e3228. https://doi.org/10.1371/journal.pone.0003228

Nor, S. M. (2001). Elevational diversity patterns of small mammals on Mount Kinabalu, Sabah, Malaysia. *Global Ecology and Biogeography*, *10*(1), 41–62. https://doi.org/10.1046/j.1466-822x.2001.00231.x

Novembre, J., & Stephens, M. (2008). Interpreting principal component analyses of spatial population genetic variation. *Nature Genetics*, *40*(5), 646–649. https://doi.org/10.1038/ng.139

Oswald, J. A., Harvey, M. G., Remsen, R. C., Foxworth, D. U., Cardiff, S. W., Dittmann, D. L., & Brumfield, R. T. (2016). Willet be one species or two? A genomic view of the evolutionary history of *Tringa semipalmata*. *The Auk*, *133*(4), 593–614. https://doi.org/10.1642/AUK-15-232.1

Payne, J., Francis, C. M., & Phillipps, K. (2016). *A field guide to the mammals of borneo*. The Sabah Society.

Peakall, R., & Smouse, P. E. (2012). GenAlEx 6.5: Genetic analysis in Excel. Population genetic software for teaching and research-an update. *Bioinformatics*, *28*(19), 2537–2539. https://doi.org/10.1093/bioinformatics/bts460

Petkova, D., Novembre, J., & Stephens, M. (2016). Visualizing spatial population structure with estimated effective migration surfaces. *Nature Genetics*, *48*(1), 94–100. https://doi.org/10.1038/ng.3464

Pierce, A. A., Gutierrez, R., Rice, A. M., & Pfennig, K. S. (2017). Genetic variation during range expansion: Effects of habitat novelty and hybridization. *Proceedings of the Royal Society B: Biological Sciences*, *284*(1852), 20170007. https://doi.org/10.1098/rspb.2017.0007

Polato, N. R., Gill, B. A., Shah, A. A., Gray, M. M., Casner, K. L., Barthelet, A., & Zamudio, K. R. (2018). Narrow thermal tolerance and low dispersal drive higher speciation in tropical mountains. *Proceedings of the National Academy of Sciences of the United States of America*, *115*(49), 12471–12476. https://doi.org/10.1073/pnas.1809326115

Pritchard, J. K., Stephens, M., & Donnelly, P. (2000). Inference of population structure using multilocus genotype data. *Genetics*, *155*(2), 945–959.

R Core Team (2019). *R: A Language and Environment for Statistical Computing*. Vienna, Austria: R Foundation for Statistical Computing. https://www.R-project.org/

Roberts, T. E., Lanier, H. C., Sargis, E. J., & Olson, L. E. (2011). Molecular phylogeny of treeshrews (Mammalia: Scandentia) and the timescale of diversification in Southeast Asia. *Molecular Phylogenetics and Evolution*, *60*(3), 358–372. https://doi.org/10.1016/j.ympev.2011.04.021

Ronquist, F., & Huelsenbeck, J. P. (2003). MrBayes 3: Bayesian phylogenetic inference under mixed models. *Bioinformatics*, *19*(12), 1572–1574. https://doi.org/10.1093/bioinformatics/btg180

Schmitz, J., Ohme, M., & Zischler, H. (2000). The complete mitochondrial genome of *Tupaia belangeri* and the phylogenetic affiliation of Scandentia to other Eutherian orders. *Molecular Biology and Evolution*, *17*(9), 1334–1343. https://doi.org/10.1093/oxfordjournals.molbev.a026417

Smith, B. T., Harvey, M. G., Faircloth, B. C., Glenn, T. C., & Brumfield, R. T. (2014). Target capture and massively parallel sequencing of ultraconserved elements for comparative studies at shallow evolutionary time scales. *Systematic Biology*, *63*(1), 83–95. https://doi.org/10.1093/sysbio/syt061

Städler, T., Haubold, B., Merino, C., Stephan, W., & Pfaffelhuber, P. (2009). The impact of sampling schemes on the site frequency spectrum in nonequilibrium subdivided populations. *Genetics*, *182*(1), 205–216. https://doi.org/10.1534/genetics.108.094904

Still, C. J., Foster, P. N., & Schneider, S. H. (1999). Simulating the effects of climate change on tropical montane cloud forests. *Nature*, *398*(6728), 608–610. https://doi.org/10.1038/19293

Sturges, H. (1926). The choice of a class-interval. *Journal of the American Statistical Association*, *21*, 65–66.

Tsai, W. L. E., Mota-Vargas, C., Rojas-Soto, O., Bhowmik, R., Liang, E. Y., Maley, J. M., & McCormack, J. E. (2019). Museum genomics reveals the speciation history of Dendrortyx wood-partridges in the mesoamerican highlands. *Molecular Phylogenetics and Evolution*, *136*, 29–34. https://doi.org/10.1016/j.ympev.2019.03.017

van der Ent, A., Cardace, D., Tibbett, M., & Echevarria, G. (2018). Ecological implications of pedogenesis and geochemistry of ultramafic soils in Kinabalu Park (Malaysia). *Catena*, *160*, 154–169. https://doi.org/10.1016/j.catena.2017.08.015

von Thaden, A., Nowak, C., Tiesmeyer, A., Reiners, T. E., Alves, P. C., Lyons, L. A., & Cocchiararo, B. (2020). Applying genomic data in wildlife monitoring: Development guidelines for genotyping degraded samples with reduced single nucleotide polymorphism (SNP) panels. *Molecular Ecology Resources*, *20*(3), 662–680. https://doi.org/10.1111/1755-0998.13136

Waits, L. P., Luikart, G., & Taberlet, P. (2001). Estimating the probability of identity among genotypes in natural populations: Cautions and guidelines. *Molecular Ecology*, *10*(1), 249–256. https://doi.org/10.1046/j.1365-294X.2001.01185.x

Waples, R. S., & Do, C. (2008). Ldne: A program for estimating effective population size from data on linkage disequilibrium. *Molecular Ecology Resources*, *8*(4), 753–756. https://doi.org/10.1111/j.1755-0998.2007.02061.x

Weiss-Lehman, C., & Shaw, A. K. (2019). Spatial population structure determines extinction risk in climate-induced range shifts. *The American Naturalist*, *195*(1), 31–42. https://doi.org/10.1086/706259

Winker, K., Glenn, T. C., & Faircloth, B. C. (2018). Ultraconserved elements (UCEs) illuminate the population genomics of a recent, high-latitude avian speciation event. *PeerJ*, *6*, e5735. https://doi.org/10.7717/peerj.5735

SUPPORTING INFORMATION

Additional supporting information may be found online in the Supporting Information section.

How to cite this article: Parker LD, Hawkins MTR, Camacho-Sanchez M, et al. Little genetic structure in a Bornean endemic small mammal across a steep ecological gradient. *Mol. Ecol.*2020;29:4074–4090. https://doi.org/10.1111/mec.15626